

文章编号:1000-0550(2024)03-0956-14

DOI: 10.14027/j.issn.1000-0550.2023.028

近千年气候环境快速变化的长江中游石笋 $\delta^{13}\text{C}$ 记录

柳静¹, 张伟宏¹, 徐昊², 邵庆丰², 卢海欣¹, 李茂霞¹, 陈剑舜²

1. 浙江师范大学地理与环境科学学院, 浙江金华 321004

2. 南京师范大学地理科学学院, 南京 210023

摘要 【目的】研究亚洲季风区中世纪气候异常期(Medieval Climate Anomaly, MCA)和小冰期(Little Ice Age, LIA)的生态水文过程及其两个阶段的转变特征,有助于进一步理解区域水文生态环境变化与季风气候之间的联系。【方法】基于长江中游湖北省永兴洞两支高分辨率石笋的 $\delta^{13}\text{C}$ 记录,采用ISCAM(Intra-Site Correlation Age Modelling)程序对这两条记录进行客观拼接,重建了该地区1044~1954 A.D.期间局地地表水文环境的变化历史。【结果】 $\delta^{13}\text{C}$ 在MCA和LIA时期表现为完全不同的两个状态, $\delta^{13}\text{C}$ 在MCA整体减小,而在LIA整体增大。此变化特征与西南以及长江中游地区众多石笋 $\delta^{13}\text{C}$ 一致,表明MCA到LIA局地地表植被呼吸活动和降水发生了从强到弱的转变。永兴洞 $\delta^{13}\text{C}$ 显示由MCA向LIA的转变过程迅速,Rampfit方法分析得出此转变过程发生在1434~1460 A.D.,持续时间为26年。永兴洞记录支持MCA向LIA的转变可能由气候变化和人类活动共同影响所致的认识。通过与其他记录对比,发现永兴洞 $\delta^{13}\text{C}$ 与太阳总辐射量、热带辐合带、我国东部温度、厄尔尼诺—南方涛动在MCA和LIA事件尺度上存在对应关系,表明过去千年长江中游地表生态水文环境和全球气候变化有着动力联系;人类活动对地表植被的影响可能与区域或全球气候变化的背景相关联。【结论】通过对过去千年永兴洞石笋 $\delta^{13}\text{C}$ 序列的研究,发现MCA与LIA的生态水文特征差异显著,其变化可能与全球气候变化和人类活动有关。该研究不仅清晰地确立了MCA与LIA在长江中游地区的时间界限,而且加深了对过去千年长江中游地区两个时期的生态水文环境变化特征及其原因的理解。

关键词 石笋;碳同位素;地表植被;转变;小冰期

第一作者简介 柳静,女,1999年出生,硕士研究生,自然地理学,E-mail: liujingis@foxmail.com

通信作者 张伟宏,女,讲师,E-mail: zhangwh@zjnu.cn

陈剑舜,男,博士,E-mail: jianshunchen@foxmail.com

中图分类号 P532 文献标志码 A

0 引言

中世纪气候异常期(Medieval Climate Anomaly, MCA)^[1]与小冰期(Little Ice Age, LIA)^[2]的气候环境变化特征对于预测未来人为成因的全球变暖环境变化至关重要。由于全球和区域气候环境变化的复杂性^[3-4],利用多种重建资料刻画MCA和LIA的区域变化特征非常必要。目前,已有众多古气候记录表征了这两个特征期在全球不同区域的起始时间和干湿特征,多数研究认为MCA发生于9—14世纪,而LIA可能发生于15—19世纪^[5-6]。然而,受重建资料以及区域差异性等因素的影响,我国不同区域气候记录显示的MCA向LIA的转变时间存在差异。例如,北方开元洞石笋记录显示MCA至LIA的转变发生于1482 A.D.^[7];而西北地区的中泉子湖记录显示这两

个特征期的转变发生于1300 A.D.^[8];在我国西南地区,泸沽湖多指标记录显示大约1300 A.D.为MCA至LIA的转变时期^[9]。在两个时期干湿变化特征方面,我国季风气候区的多数研究认为普遍存在南北偶极型的降水模式,MCA和LIA时期南北方大致呈现相反的干湿格局,即MCA时北方湿润,南方干旱,而LIA时北方干旱,南方湿润^[10-12],表现出显著的季风降水空间差异。但某些局部区域的干湿特征在两个气候特征期的表现并非所期望的那样^[13-14]。而造成此种气候特征变化的原因可能是太阳活动外部驱动与地球内部变化如热带辐合带(Intertropical Convergence Zone, ITCZ)、厄尔尼诺—南方涛动(El Niño-Southern Oscillation, ENSO)等因素共同作用的结果^[10,15-16]。因此,进一步细化明确MCA和LIA在小

收稿日期:2022-11-16;修回日期:2023-03-28;录用日期:2023-05-08;网络出版日期:2023-05-08

基金项目:浙江省自然科学基金项目(LY20D020001)[Foundation: Natural Science Foundation of Zhejiang Province, No. LY20D020001]

区域尺度上发生时间和空间特征的异同性,厘清MCA和LIA的时空变化特征,有助于提高对这两个气候特征期动力机制的理解和对未来气候变化的预测。

过去着重利用石笋代用指标中的 $\delta^{18}\text{O}$ 重建气候环境的变化,多数研究认为 $\delta^{18}\text{O}$ 主要反映了夏季风整体强度的变化,并非洞穴地点的水文环境变化^[10,17]。局域生态环境特征与区域水文气候变化紧密联系,近年来已有大量研究表明石笋 $\delta^{13}\text{C}$ 在重建局域生态环境和水文气候上具有潜力^[18-21]。我国不同区域石笋研究均有报道石笋 $\delta^{13}\text{C}$ 与局域水文气候存在密切联系,能够较好地反映局域生态环境演化。最近,西北万象洞石笋 $\delta^{13}\text{C}$ 在数十年—百年尺度上主要与区域水文相关的土壤湿度平衡和植被密度有关^[20];而东南地区多个洞穴石笋 $\delta^{13}\text{C}$ 研究表明 $\delta^{13}\text{C}$ 能够较好地反映长江中下游区域的旱涝特征,结合石笋高精度定年和高分辨率的特征,进一步明确古文化演化阶段与水文气候变化之间的联系^[22]。此外,长江中游地区和西南地区多个洞穴石笋 $\delta^{13}\text{C}$ 的研究均表明 $\delta^{13}\text{C}$ 能很好地响应于局域水文气候的变化,进而表征洞穴区域生态环境演化^[18,23]。因此,石笋 $\delta^{13}\text{C}$ 记录是 $\delta^{18}\text{O}$ 记录表征季风水循环的有效补充,二者从不同侧面反映季风水循环的变化过程。而对于MCA和LIA的气候特征变化,石笋 $\delta^{13}\text{C}$ 的研究也将有助于进一步提升对两个气候特征期的理解。例如,陈朝军等^[11]利用贵州地区多支石笋 $\delta^{13}\text{C}$ 记录探究了过去2 000年以来西南地区洞穴上部地表生态环境的变化,发现 $\delta^{13}\text{C}$ 从MCA至LIA持续偏重,认为气候变化与人类南迁的共同影响导致了该地区石漠化的扩张。然而,在南方与北方交界的长江中游地区,MCA和LIA的气候环境特征还存在争议^[24-25],MCA向LIA的转变时间尚未明确。此外,长江中游与贵州地区的石笋 $\delta^{13}\text{C}$ 记录在MCA和LIA时期是否一致变化,在一定程度上可以验证人类南迁导致地表环境变化的认识。

选用湖北省永兴洞两支高分辨率石笋 $\delta^{13}\text{C}$ 记录,探讨MCA和LIA的气候环境特征,刻画MCA向LIA的转变时间和特征,并通过与其他记录对比尝试理解MCA与LIA时期长江中游地区气候环境变化的原因。该研究对进一步明确我国MCA与LIA的气候环境时空分布特征有一定的补充意义。

1 区域概况、材料与方法

采用部分时段重叠的两支石笋(YX262和YX275)^[26-28],这两支石笋采自湖北省神农架保康县歇马镇永兴洞(31°35' N, 111°14' E; 洞口海拔高度约800 m)。洞穴上覆植被为多年生木本和灌木丛草本^[26-27,29],洞内温度为14℃,相对湿度接近100%^[30-31]。该洞地处亚热带季风气候区,夏季受来自低纬的水汽影响显著。1981—2010年保康县降水记录显示,此区域年均降水量约930 mm,70%的降水主要分布在夏季风盛行的5—9月^[29]。

YX262和YX275石笋均采集于洞穴深部,长度分别为159 mm和120 mm,主要由方解石构成。两支石笋的碳氧同位素及年代样品的取样及相关测试方法见文献[26]和[28]。肉眼观察和U/Th年龄显示这两支石笋沉积连续,不存在明显的沉积间断^[26-28]。已报道的氧同位素在重叠时段有较好的重现性^[26,28](图1a),暗示两石笋在沉积过程中同位素分馏平衡,受非气候因素影响较小^[26,32],可用于重建古气候环境演变。

2 结果

2.1 年代

YX262和YX275石笋共测定了13个U/Th年龄^[26,28]。整体上,两支石笋²³⁸U含量较高,²³²Th含量偏低,导致测年误差较小,为4~19年。为了更好地拼接两支石笋记录,二者时标均由Mod-Age模式^[33]建立(图2)。年龄—深度模型结果显示,YX262沉积于1 027~1 639 A.D.,持续时间约612年,平均分辨率为3.8年;YX275沉积于1 361~1 955 A.D.,持续时间约594年,平均分辨率为5年。此外,模型结果显示这两支石笋生长速率均较为匀速(图2),说明同位素曲线变化形态及其所指示的局域地表环境和气候变化受测试年龄数目的影响较小。

2.2 石笋 $\delta^{13}\text{C}$ 与 $\delta^{18}\text{O}$ 记录

分别测试了YX262和YX275石笋120组和159组碳氧同位素数据^[26-28],并将未报道的YX262 $\delta^{13}\text{C}$ 数据和已报道的同位素数据结合,研究了长江中游地区气候环境变化及可能的驱动机制。鉴于两支石笋的碳氧同位素记录在重叠时段呈现出较好的一致性,为消除不同记录间相对幅度变化的偏差以获取更长时间序列的综合记录,利用ISCAM(Intra-Site

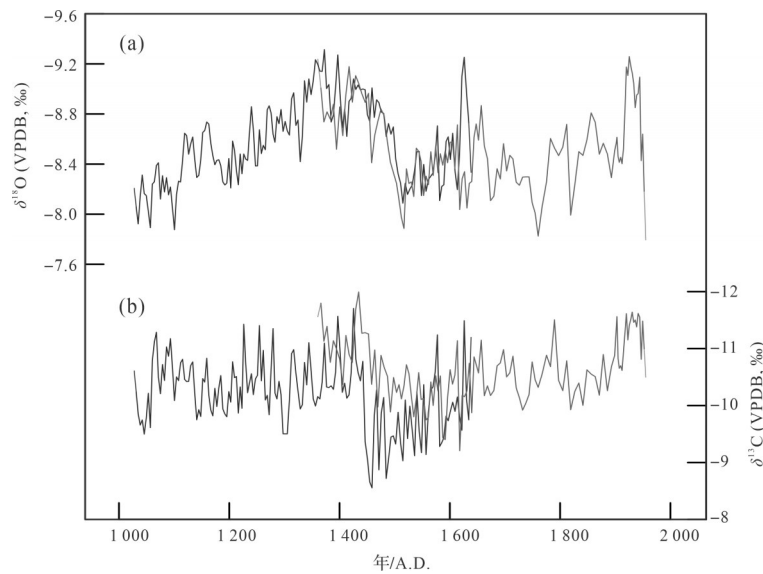


图1 两支石笋的氧碳同位素记录

(a)黑色和灰色实线分别表示YX262和YX275石笋 $\delta^{18}\text{O}$ 记录;(b)黑色和灰色实线分别表示YX262和YX275石笋 $\delta^{13}\text{C}$ 记录

Fig.1 Oxygen and carbon isotope records of two stalagmites in Yongxing cave
 $\delta^{18}\text{O}$ and $\delta^{13}\text{C}$ records of stalagmites YX262 (black) and YX275 (gray)

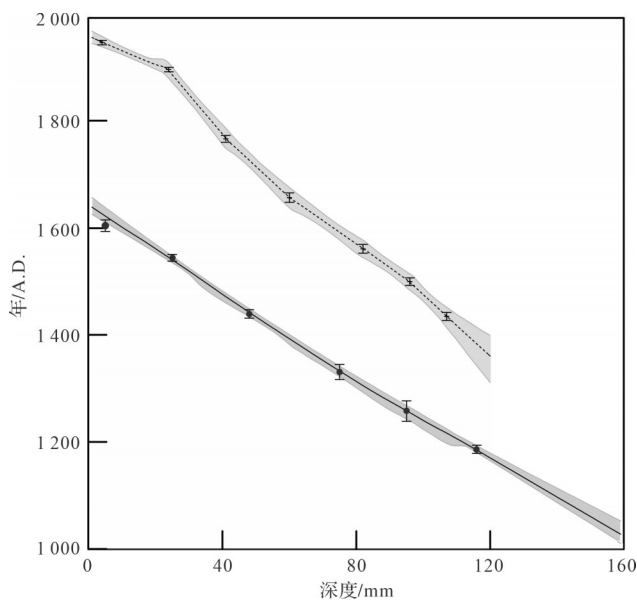


图2 YX262和YX275年龄模式图

黑色虚线和黑色实线分别为YX275和YX262的年龄模式;灰色条带为95%置信度范围,黑色加号和圆点表示年龄点,计算误差为 $\pm 2\sigma$

Fig.2 Age models for the YX262 and YX275 $\delta^{13}\text{C}$ records

The black dashed and solid lines represent the modeled age frames for YX275 and YX262, respectively; Gray bands are 95% confidence levels; Plus and dot symbols indicate ^{230}Th dates with $\pm 2\sigma$ error bars

Correlation Age Modelling)程序^[34],分别将这两支石笋的 $\delta^{13}\text{C}$ 与 $\delta^{18}\text{O}$ 序列进行拼接(图3)。此程序能够有效地消除不同石笋同位素记录之间人工拼接时相对幅度变化的差异,有助于研究拼接记录在不同时间段的相对幅度变化。

拼接合成的 $\delta^{13}\text{C}$ 与 $\delta^{18}\text{O}$ 记录的时间跨度为1044~1954 A.D.,共持续910年,包含MCA和LIA两个气候特征期。 $\delta^{18}\text{O}$ 值在 -9.24‰ 和 -7.79‰ 之间波动,变幅为 1.45‰ ,平均值为 -8.50‰ 。 $\delta^{18}\text{O}$ 值在MCA时期较LIA整体偏负,在MCA内部, $\delta^{18}\text{O}$ 呈现逐渐负偏特征,LIA期间 $\delta^{18}\text{O}$ 显示出明显的数十年—百年尺度的振荡^[26](图3a);相对于 $\delta^{18}\text{O}$, $\delta^{13}\text{C}$ 的变化幅度较大,达 2.78‰ 。 $\delta^{13}\text{C}$ 在 -12.12‰ ~ -9.34‰ 范围内波动,平均值为 -10.77‰ 。 $\delta^{13}\text{C}$ 较为明显的特征是,在MCA向LIA转变的时期,其值呈现出明显的均值突变。在MCA时期, $\delta^{13}\text{C}$ 值相对偏负,虽然存在数十年尺度的振荡,但并未呈现出明显的长期趋势。而在LIA时期, $\delta^{13}\text{C}$ 值相对偏正,也未呈现出显著的变化趋势(图3b)。总体而言, $\delta^{13}\text{C}$ 与 $\delta^{18}\text{O}$ 变化较为相似,均显示MCA时整体负偏,而LIA时整体正偏。然而不同的是,MCA时期二者的变化趋势存在差异, $\delta^{18}\text{O}$ 呈现逐渐偏负的特征,而 $\delta^{13}\text{C}$ 在 -11.08‰ 附近上下波动(图3)。

3 讨论

3.1 石笋 $\delta^{13}\text{C}$ 的气候意义

随着洞穴监测以及模拟技术不断发展,石笋 $\delta^{13}\text{C}$ 被证明对局域生态环境与气候的响应十分敏感^[36-37]。在不同时间尺度上,石笋 $\delta^{13}\text{C}$ 所反映的气候环境特点

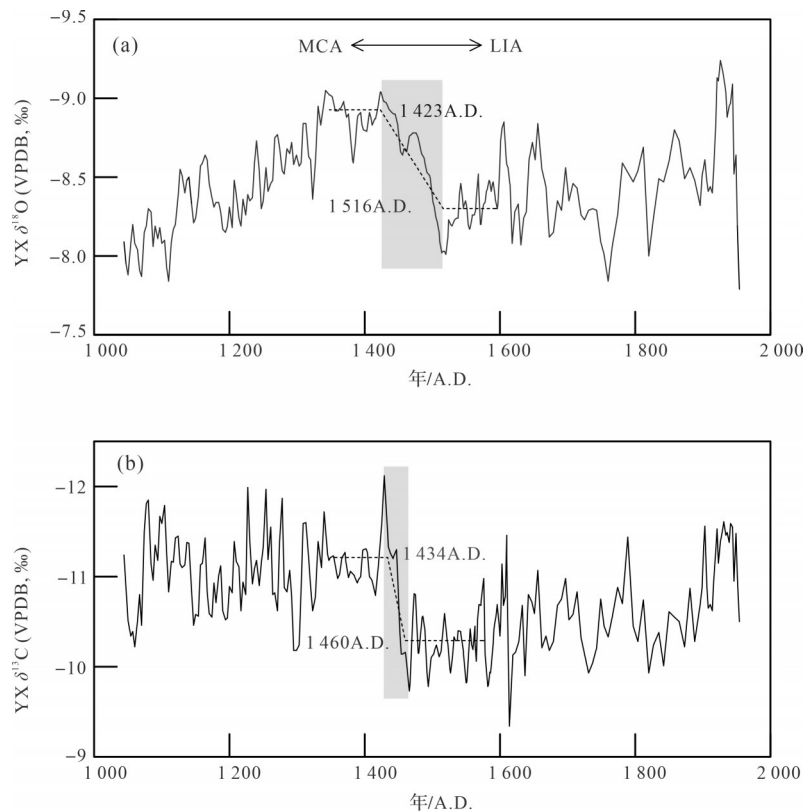


图3 永兴洞两支石笋的氧碳同位素合成记录

(a)合成的 $\delta^{18}\text{O}$; (b)合成的 $\delta^{13}\text{C}$; 虚线表示 Rampfit^[35]分析的MCA向LIA转变结果; 灰色条带表示转变的持续时间

Fig.3 Composites of oxygen and carbon isotope records of stalagmites YX262 and YX275 in Yongxing cave

(a) $\delta^{18}\text{O}$ composite; (b) $\delta^{13}\text{C}$ composite; The dashed line represents the analyses of the transition from the MCA to the LIA based on the Rampfit technique^[35]; the gray bar represents the duration of the transition

存在差异,轨道尺度上石笋 $\delta^{13}\text{C}$ 的变化主要是由植被类型的自然更替而引起的^[38],而在千年—百年尺度上石笋 $\delta^{13}\text{C}$ 的变化可能与局域生态水文环境有关^[11,18,20]。此外,区域的差异性以及沉积过程的复杂性也使得石笋 $\delta^{13}\text{C}$ 在不同的背景下产生一定的差别^[39-40]。在长江中游地区,牛洞^[23]、落水洞^[41]、玉龙洞^[21]、和尚洞^[42]等众多的洞穴石笋 $\delta^{13}\text{C}$ 被认为是局域生态环境和水文气候变化的重要代用指标。因此,同区域的永兴洞石笋 $\delta^{13}\text{C}$ 可能同样反映了局域生态水文环境的变化。即当降水量丰富时,植被生长茂盛,密度大,植物根系的呼吸作用和微生物活动增强,生物量增加,土壤 CO_2 产率增大,促使土壤中 ^{12}C 相对富集,土壤富集的 ^{12}C 通过雨水的溶解,形成 $\text{Ca}(\text{HCO}_3)_2$ 溶液,致使石笋 $\delta^{13}\text{C}$ 值偏负^[39,43-44]。此外,降水量大时引起水—岩相互作用的时间缩短,围岩($\delta^{13}\text{C}$ 值较重)溶解变少,石笋 $\delta^{13}\text{C}$ 亦相对负偏^[27,44]。反之,降水量减少时,植被生物量的减少以及围岩溶解的增加均导致石笋 $\delta^{13}\text{C}$ 的正偏。

石笋 $\delta^{13}\text{C}$ 与文献资料的对比,进一步证实了石笋 $\delta^{13}\text{C}$ 变化与局地水文环境变化的关联性。永兴洞石笋 $\delta^{13}\text{C}$ 与历史资料重建的宜昌地区近500年来的旱涝指数序列具有很好的一致性^[45](图4a)。因永兴洞数据平均分辨率约为4.4年,而旱涝指数时间序列的分辨率为1年,因而通过等间距内插将这两个序列的分辨率统一调整为4年,再进行5点滑动平均。相关性计算结果表明,石笋 $\delta^{13}\text{C}$ 与旱涝指数的相关性达0.56($N=116, P<0.01$)。如图4a所示,当旱涝指数小于3时,表示宜昌地区较为湿润,对应石笋 $\delta^{13}\text{C}$ 偏负;而当旱涝指数大于3时,表示宜昌地区较为干旱,对应石笋 $\delta^{13}\text{C}$ 偏正。石笋 $\delta^{13}\text{C}$ 能够反映局地水文环境的变化还得到石笋生长速率的支持, $\delta^{13}\text{C}$ 负偏时石笋的生长速率较快,而 $\delta^{13}\text{C}$ 正偏时石笋的生长速率较慢(图4b)。如石笋YX262的生长速率从MCA至LIA表现出明显的递减模式。此外,永兴洞石笋 $\delta^{13}\text{C}$ 和 $\delta^{18}\text{O}$ 在年代尺度上存在较好的相关性($R=0.46, N=279, P<0.01$),暗示 $\delta^{13}\text{C}$ 和 $\delta^{18}\text{O}$ 的变化可能具有相同的强迫

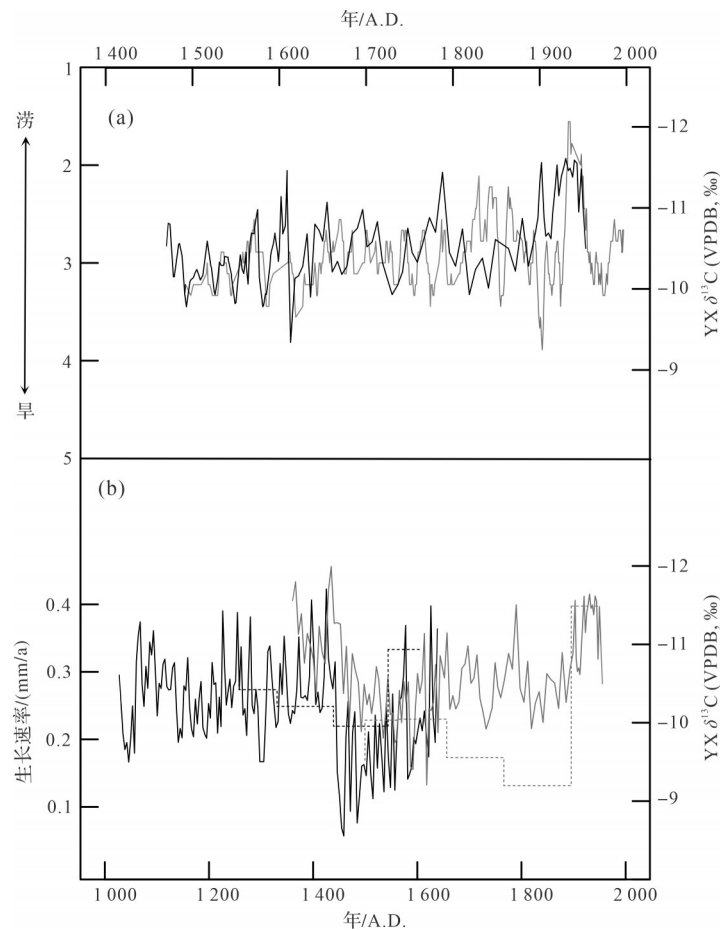


图4 石笋 $\delta^{13}\text{C}$ 与旱涝指数和生长速率对比

(a) 灰色线为平滑了5点的宜昌旱涝指数^[45](1.涝, 2.偏涝, 3.正常, 4.偏旱, 5.旱), 黑色线为永兴洞石笋 $\delta^{13}\text{C}$ 合成记录; (b) 黑色和灰色实线分别为YX262和YX275石笋 $\delta^{13}\text{C}$ 记录; 黑色虚线和灰色虚线分别为YX262和YX275的生长速率

Fig.4 Comparison of stalagmite $\delta^{13}\text{C}$ records with drought/flood index at Yichang and growth rates

(a) The drought/flood index in Yichang after 5 points of smoothing (gray)^[45] and the stalagmite $\delta^{13}\text{C}$ composite record in Yongxing cave (black); (b) The YX262 (black) and YX275 (gray) $\delta^{13}\text{C}$ records; The black and gray dashed lines represent the growth rate of YX262 and YX275, respectively

机制。尽管对石笋 $\delta^{18}\text{O}$ 的理解还未取得一致看法^[46], 但最近研究成果显示石笋 $\delta^{18}\text{O}$ 主要反映了大尺度季风环流及其影响的降水变化^[47]。基于以上论证, 永兴洞石笋记录很可能受局域水文气候变化的影响。然而, 除自然因素影响外, 一些洞穴石笋 $\delta^{13}\text{C}$ 值在数十年或数百年尺度的突然增大与人类活动有关, 人口增加、森林砍伐、土地垦殖等会改变土壤有机环境, 从而影响石笋 $\delta^{13}\text{C}$ 的变化^[48-49]。Zhang *et al.*^[48]基于我国东部两支石笋 $\delta^{13}\text{C}$ 的研究, 发现在700~1 100 A.D. $\delta^{13}\text{C}$ 的异常增大与安史之乱爆发后人口大量南迁有关, 人类的毁林开荒改变了地表的生态环境, 促使 $\delta^{13}\text{C}$ 增大。

3.2 MCA和LIA的水文环境变化与转变特征

永兴洞石笋 $\delta^{13}\text{C}$ 序列显示MCA与LIA时期呈现出两种完全不同的气候特征。MCA时期石笋 $\delta^{13}\text{C}$ 整

体偏负, 而LIA时期整体偏正(图5a)。这与陈朝军等^[11]研究的西南地区石将军洞石笋 $\delta^{13}\text{C}$ 具有一定的相似性(图5b)。此外, 同属于长江中游地区的湖北犀牛洞^[50]、落水洞^[51]以及湖南莲花洞^[52]石笋 $\delta^{13}\text{C}$ 均显示了MCA时期偏负而LIA偏正的特点(图5c~e)。虽然这些记录在数十年—一百年尺度的振荡上存在差异, 但仍然能够辨别各个记录在MCA与LIA时期不同的气候特征。

依据上文对石笋 $\delta^{13}\text{C}$ 的理解, MCA与LIA时期不同的气候特征呈现了该地区清晰的水文环境变化。MCA时期 $\delta^{13}\text{C}$ 平均值为 -11.1‰ , 整体负偏; LIA时期 $\delta^{13}\text{C}$ 平均值为 -10.4‰ , 整体正偏, 表明长江中游地区存在湿润的MCA和相对干旱的LIA(图6)。长江中游其他记录也呈现了相似的气候环境变化特征。利用多指标以及数学模型建立的中国中部地区夏季降

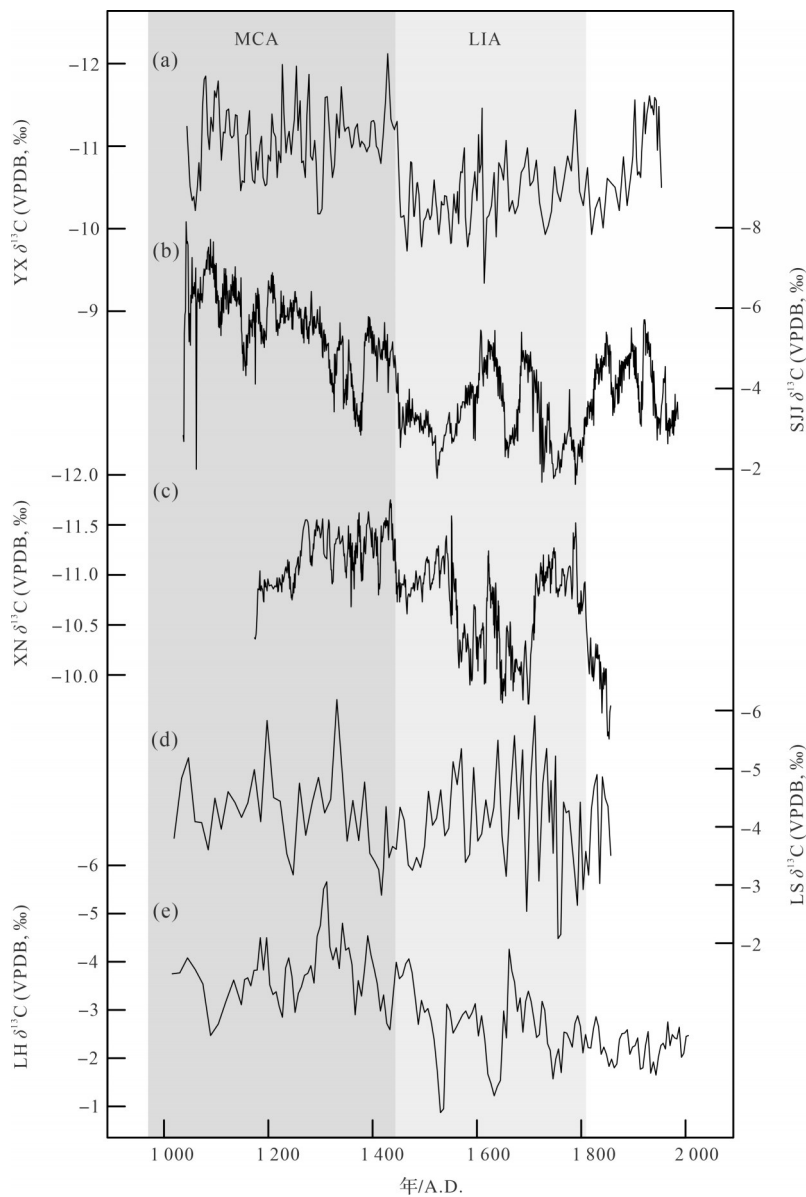


图5 不同洞穴石笋 $\delta^{13}\text{C}$ 记录对比

(a)湖北永兴洞石笋 $\delta^{13}\text{C}$; (b)贵州石将军洞石笋 $\delta^{13}\text{C}$ ^[11]; (c)湖北犀牛洞石笋 $\delta^{13}\text{C}$ ^[50]; (d)湖北落水洞石笋 $\delta^{13}\text{C}$ ^[51]; (e)湖南莲花洞石笋 $\delta^{13}\text{C}$ ^[52];深灰色条带为MCA;浅灰色条带为LIA

Fig.5 Comparison of stalagmites $\delta^{13}\text{C}$ records from different caves

Compared $\delta^{13}\text{C}$ records are from (a) Yongxing cave, Hubei; (b) Shijiangjun cave, Guizhou^[11]; (c) Xiniu cave, Hubei^[50]; (d) Luoshui cave, Hubei^[51]; (e) Lianhua cave, Hunan^[52]; the dark and light grey bands represent MCA and LIA, respectively

水量变化记录^[53]显示(图6),月降水量变化的平均值在MCA时期为4.6 mm,在LIA时期为3.0 mm,指示MCA时期长江中游地区水文气候较为湿润,而LIA时期相对干旱。该水文环境变化特征也得到植物孢粉证据的支持。江西玉华山乔灌木花粉百分比^[54]在MCA时较大,而LIA时较小,表明MCA时较为湿润,LIA则与此相反(图6)。此外,湖北地区岩心中的植物生态记录^[57]同样支持了此观点。尽管过去研究显

示我国南北方MCA和LIA呈现出相反的降水格局,北方MCA湿润而LIA干旱^[10,58],南方MCA干旱而LIA湿润^[12]。然而,位于我国南北方过渡带的湖北石笋 $\delta^{13}\text{C}$ 显示出与北方类似的水文环境变化。需要指出的是,与永兴洞石笋 $\delta^{13}\text{C}$ 记录反向的水文环境模式也在长江流域有所报道。如湖北大九湖^[25]和浙江千亩田泥炭记录^[59]显示了干旱的MCA和湿润的LIA,而这种差异可能与山地海拔效应以及MCA和LIA时期不

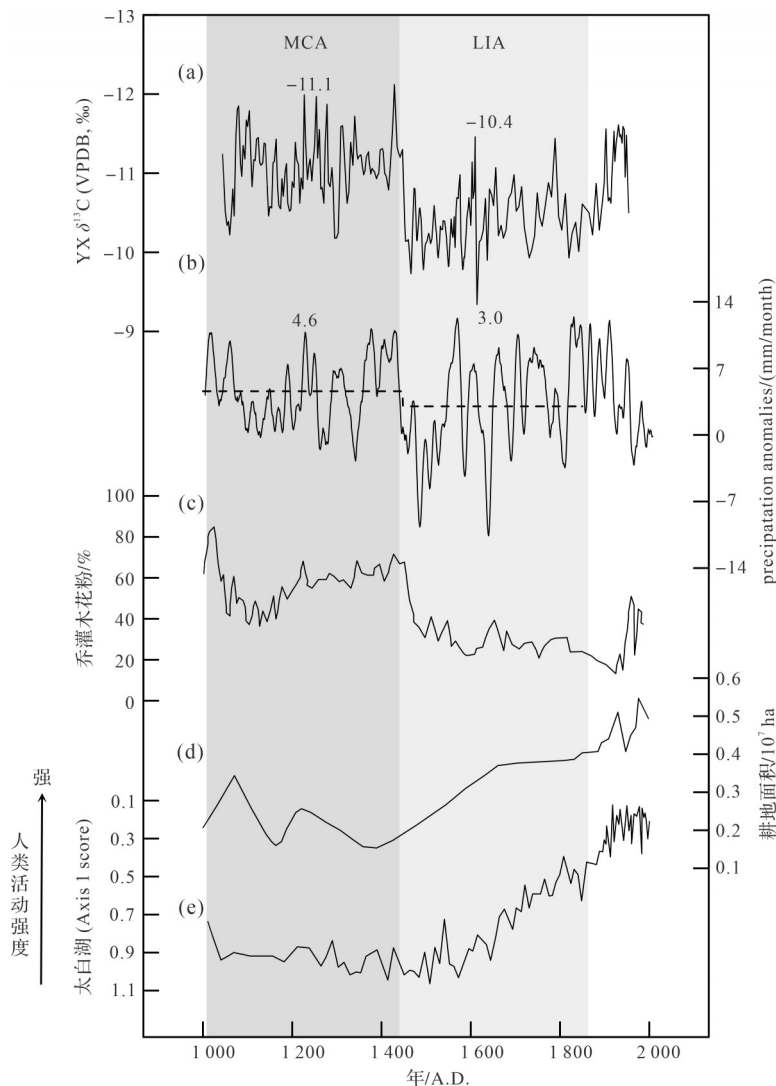


图6 永兴洞石笋 $\delta^{13}\text{C}$ 与长江中下游其他记录对比

(a) 永兴洞石笋 $\delta^{13}\text{C}$; (b) 11年滑动平均的中国中部地区夏季降水变化^[53]; (c) 江西玉华山乔灌木花粉^[54]; (d) 湖北耕地面积^[55]; (e) 太白湖 axis 1 score^[56]; 深灰色条带表示MCA, 浅灰色条带表示LIA; 黑色虚线及对应数字代表MCA与LIA两个阶段的平均值

Fig.6 Comparison of the stalagmites $\delta^{13}\text{C}$ record in Yongxing cave with other records in the middle and lower reaches of the Yangtze River

(a) stalagmite $\delta^{13}\text{C}$ composite record from Yongxing cave; (b) 11-year moving average of summer precipitation anomalies in central China^[53]; (c) tree and shrub pollen record from Yuhua mountain, Jiangxi province^[54]; (d) cultivated land area in Hubei province^[55]; and (e) axis 1 score derived from multiple proxy in Taibai lake^[56]; The dark and light grey bands represent MCA and LIA, respectively; the black dashed lines show the averaged condition for MCA and LIA

同的气温背景^[60]有关。大九湖盆地海拔高度介于1700~1760 m^[61], 千亩田海拔高度约为1338 m^[59], 两地海拔高度均显著高于永兴洞(800 m)。可能在MCA时期, 较高的北半球气温引起大气水汽含量显著增加, 在山地低海拔区域受地形雨的影响更易形成降水; 而在LIA时期, 较低的北半球气温造成大气水汽含量降低, 在山地高海拔区域受地形雨的影响更为显著。此外, LIA时高海拔区域气温低, 蒸发弱, 湿度高, 可能在一定程度上造成这些记录呈现出与永兴洞相反的降水模式。

永兴洞石笋 $\delta^{13}\text{C}$ 清晰地记录了MCA向LIA的快速转变特征和起止时间。利用Rampfit算法^[35]对永兴洞石笋碳氧同位素记录进行了趋势变化分析(图3), 结果显示, 永兴洞石笋 $\delta^{13}\text{C}$ 与 $\delta^{18}\text{O}$ 在MCA向LIA转变时有明显的快速变化, 但存在差异。MCA向LIA转变期间, 石笋 $\delta^{18}\text{O}$ 迅速偏正1.01‰, 时间跨度为1423~1516 A.D., 中间点年龄为1469 A.D., 持续时间为93年(图3a); 石笋 $\delta^{13}\text{C}$ 显示此转变开始于1434 A.D., 结束于1460 A.D., 中间点年龄为1447 A.D., 持续时间为26年, 变化幅度达1.31‰(图3b)。 $\delta^{13}\text{C}$

的均值突变晚于 $\delta^{18}\text{O}$ 变化约10年,可能反映了局地生态水文状况对大尺度大气环流的调整和响应。 $\delta^{13}\text{C}$ 的快速变化和其在MCA和LIA期完全不同的均值状态,暗示了长江中游地区MCA与LIA的划分界线约在1447 A.D.

MCA至LIA水文状态的快速转变除了受气候变化影响外,人类活动的影响也不容忽视。Lan *et al.*^[8]基于季风边缘区的多指标记录,认为季风强度在MCA向LIA转变期的快速减弱是对太阳总辐照度减小及其引起的大气环流变化的非线性响应。而在人类活动影响方面,永兴洞石笋 $\delta^{13}\text{C}$ 的快速转变可能与明朝洪武三年(1370 A.D.)至永乐十五年(1417 A.D.)发生的明初大移民事件相关,其中“江西填湖广”的移民活动规模极大^[62]。大量的移民涌入湖北,必然造成大规模的森林砍伐和土地开垦,从而改变了地表植被生态环境,最终造成了区域性的 $\delta^{13}\text{C}$ 突然偏重^[11]。历史文献资料重建的湖北省耕地面积的变化也支持人类活动加强的认识。如图6所示,1400 A.D.左右湖北省耕地面积快速增加^[55],可能是大量的人口涌入使得粮食的需求量增大,土地垦殖面积增加^[62]。同样,Xiao *et al.*^[56]利用湖北太白湖沉积物多指标记录,基于数理统计的去趋势对应分析方法,所得的轴1得分被认为是人类活动强度的指标,即轴1得分的降低反映了人类活动的增强。结合花粉及碳屑指标记录,认为1320 A.D.之前植被的变化主要受控于气候变化,而1320 A.D.之后多指标记录显示了人类活动的增强(图6)。虽然此记录显示的人类活动增强的时间与永兴洞石笋记录的突变时间不完全一致,可能与各记录年代的不确定性有关,但该记录清晰地显示14—15世纪人类活动不断增强。此外,人类活动对地表环境的影响还表现在长江中游的江西和生态环境较脆弱的贵州喀斯特地区^[11,48],研究表明人类大规模的开垦种田,加剧了地表生态环境的改变甚至导致石漠化。因此, $\delta^{13}\text{C}$ 在MCA向LIA的快速转变特征可能是在自然响应的基础上叠加了人为因素的影响。

3.3 水文环境变化的潜在驱动力

长江中游水文环境的变化与地球内外部的驱动因素有关。太阳活动外部驱动的变化对气候环境产生重要的影响^[17,63],并通过地球内部系统的反馈作用影响全球^[23,64-65]。最直观的表现是太阳活动驱动温度变化,太阳活动的强弱使得地球表面接收到不同程度的能量,由于海陆热力性质的差异使得两者的增

温幅度在太阳辐射较强时区别更加明显,温度梯度大,从而造成大气环流的改变^[50]。对比永兴洞石笋 $\delta^{13}\text{C}$ 与太阳总辐照度^[66]以及中国东部温度距平变化^[67],发现三者存在明显的对应关系,即MCA时期太阳总辐照度整体偏大,而LIA时较小(图7),分别对应于石笋 $\delta^{13}\text{C}$ 值较小和较大时期。采用Past3软件对合成的永兴洞石笋 $\delta^{13}\text{C}$ 进行功率谱分析,发现在95%置信水平下存在显著的186年的周期(图8),接近于太阳活动的双百年周期^[70]。此外,若将中国东部温度距平变化记录向年轻移动约40年,石笋 $\delta^{13}\text{C}$ 与其具有更强的相关性($R=-0.527, N=228, P<0.01$)(图7),可见永兴洞石笋 $\delta^{13}\text{C}$ 似乎滞后于温度的变化,这或许与区域植被环境对气温的响应过程有关。总体上,三者百年尺度上的对应关系支持了太阳总辐照度的强弱及其影响下的气温变化在驱动亚洲夏季风区的水文变化中扮演了重要的角色。太阳活动变化通过改变季风环流下垫面的热力性质而引起局域水文变化。当太阳辐照度强且气温较高时,海陆温度梯度的增大使得季风环流增强,降水量增加,土壤植被生长茂盛,生物量丰富,石笋 $\delta^{13}\text{C}$ 偏负。

大气以及海洋环流对长江中游水文气候变化也存在一定的影响。在地球内部因素驱动中,ITCZ移动位置以及ENSO波动也是气候变化的重要调节器^[15,28,71]。ITCZ在太阳活动的变化下发生南北移动,使得大气环流发生变化进而影响到区域性的水文状况^[72]。当ITCZ北移时,季风环流增强,大量的海洋水汽被输送到陆地而造成了大陆降水量的增加,反之亦然。通过对比发现,在百年尺度上,永兴洞石笋 $\delta^{13}\text{C}$ 记录所反映的水文环境的变化可能与ITCZ移动指数^[68]存在一定的对应关系(图7)。MCA时ITCZ的移动指数整体负偏,ITCZ位置偏北;LIA时ITCZ的移动指数整体正偏,ITCZ位置偏南。即MCA时期长江中游降水量增加,LIA时则减小,水文环境的改变使得区域植被密度及土壤 CO_2 产率发生变化,石笋 $\delta^{13}\text{C}$ 发生改变。ENSO主要通过改变海气环流过程进而影响气候^[73]。Moy *et al.*^[69]通过分析厄瓜多尔Laguna Pallcacocha沉积物红度重建了过去12 ka ENSO的活动历史,发现MCA时期出现高频厄尔尼诺现象,LIA则处于厄尔尼诺低频时期(图7),这似乎与永兴洞石笋记录相吻合。Yan *et al.*^[74]重建的南方涛动指数(Southern Oscillation Index, SOI)同样认为MCA时期为厄尔尼诺态,而LIA时期为拉尼娜态。厄尔尼诺时

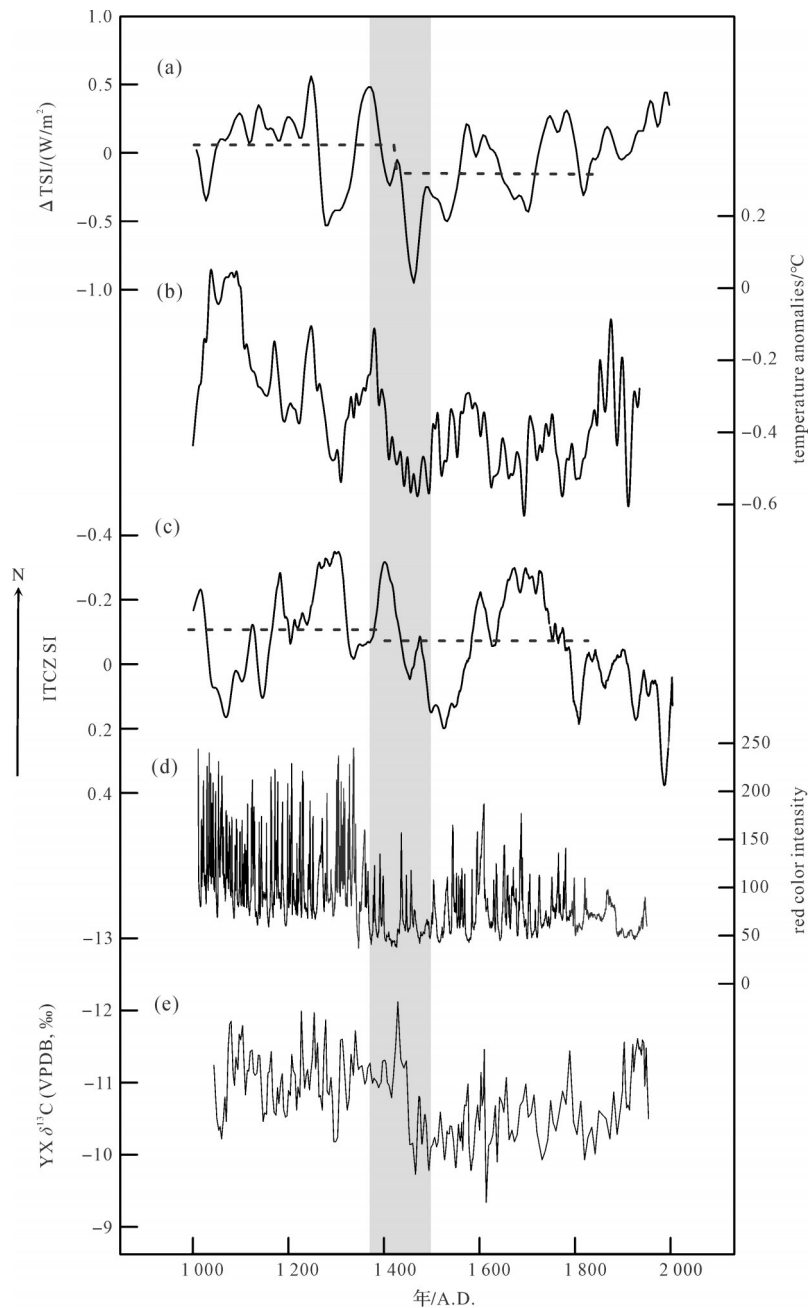


图7 永兴洞石笋 $\delta^{13}\text{C}$ 与区域或全球记录的对比

(a)太阳总辐照度^[66]; (b)重建的中国东部温度距平变化^[67]; (c)ITCZ移动指数^[68]; (d)Laguna Pallacocha 沉积物红度^[69]; (e)永兴洞石笋 $\delta^{13}\text{C}$; 黑色虚线代表太阳总辐射的平均值; 灰色虚线代表ITCZ移动指数的平均值; 灰色条带代表MCA至LIA的转变阶段

Fig.7 Comparison of the stalagmite $\delta^{13}\text{C}$ record in Yongxing cave with other records reflecting regional or global climate change

(a) total solar radiation^[66]; (b) temperature anomalies in eastern China^[67]; (c) ITCZ shift index^[68]; (d) red color intensity for the sediment from Laguna Pallacocha^[69]; (e) stalagmite $\delta^{13}\text{C}$ record in Yongxing cave; The dashed lines represent averaged conditions for the total solar radiation (black) and ITCZ shift index (gray) respectively; The gray band represents the transition from MCA to LIA

期, 中东太平洋海温异常升高, 使得该地区气压降低, 而相对应的西太平洋暖池区域气压增强, 造成了沃克环流减弱以及上升支东移, 西太平洋副热带高压偏南西伸而强, 长江中游地区受梅雨锋控制降水量丰富; 反之拉尼娜时期, 中东太平洋的气压增强对

应的西太平洋暖池气压降低, 使得沃克环流增强, 西太平洋副热带高压偏北东缩而弱, 长江中下游地区降水较少^[46,65]。可见, ITCZ和ENSO波动是驱动长江中游地区季风和人文环境变化的重要内部因素。值得一提的是, 如图7灰色条带所示, 在MCA向LIA快

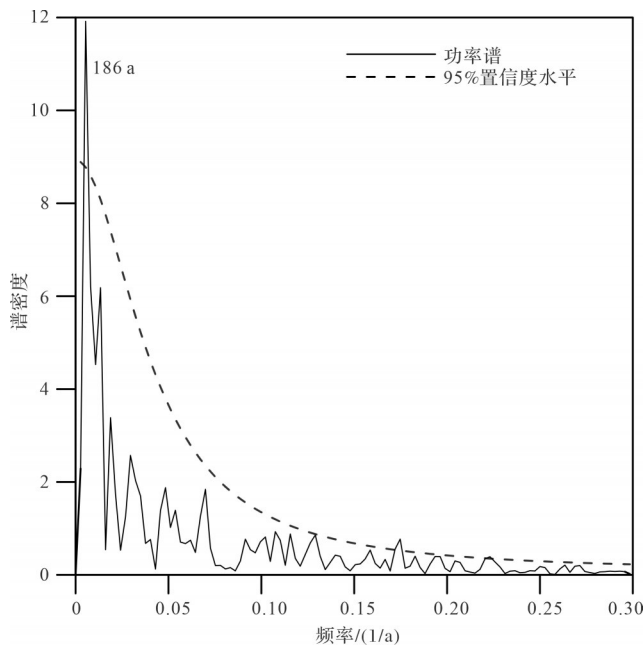


图8 永兴洞石笋 $\delta^{13}\text{C}$ 功率谱图

灰色虚线为95%置信度水平

Fig.8 Power spectral analysis of the $\delta^{13}\text{C}$ record in Yongxing cave

The gray dashed line is the 95% confidence level

速转变时期,太阳总辐照度、温度、ITCZ以及ENSO等也表现出平均状态的快速变化,表明在海气耦合过程中,地球内外部驱动以不同的形式共同参与调控了长江中游地区水文环境的改变^[75]。

4 结论

(1) 长江中游湖北永兴洞石笋 $\delta^{13}\text{C}$ 记录在MCA和LIA表现为完全不同的两个状态:MCA期 $\delta^{13}\text{C}$ 值整体偏负,而LIA期整体偏正。表明近千年该地区的水文格局发生了显著变化,MCA时期较为湿润,而LIA时期相对干旱。

(2) 在MCA向LIA的转变过程中,石笋 $\delta^{13}\text{C}$ 记录显现出明显的均值突变,发生时间为1434~1460 A.D.,持续时间26年。

(3) 近千年永兴洞 $\delta^{13}\text{C}$ 记录显示的MCA和LIA之间不同的水文环境特征,可能受自然与人为因素共同控制。其在百年尺度上不仅与太阳活动和温度有关,而且还受到ITCZ和ENSO的影响,表明太阳活动及海气耦合系统对长江中游水文循环的重要调控作用。

致谢 感谢审稿专家及编辑部老师提出的建设性修改意见,使得文章更加完善。

参考文献 (References)

- [1] Mann M E, Zhang Z H, Rutherford S, et al. Global signatures and dynamical origins of the Little Ice Age and Medieval Climate Anomaly[J]. *Science*, 2009, 326(5957): 1256-1260.
- [2] Matthes F E. Report of committee on glaciers, April 1939[J]. *Eos, Transactions American Geophysical Union*, 1939, 20(4): 518-523.
- [3] 郑景云,刘洋,郝志新,等. 过去2000年气候变化的全球集成研究进展与展望[J]. *第四纪研究*, 2021, 41(2): 309-322. [Zheng Jingyun, Liu Yang, Hao Zhixin, et al. State-of-art and perspective on global synthesis studies of climate change for the past 2000 years[J]. *Quaternary Sciences*, 2021, 41(2): 309-322.]
- [4] 高建慧,刘健,王苏民. 中国中世纪暖期气候研究综述[J]. *地理科学*, 2006, 26(3): 376-383. [Gao Jianhui, Liu Jian, Wang Sumin. Overview on studies of Medieval Warm Period in China[J]. *Scientia Geographica Sinica*, 2006, 26(3): 376-383.]
- [5] 郑景云,刘洋,吴茂炜,等. 中国中世纪气候异常期温度的多尺度变化特征及区域差异[J]. *地理学报*, 2019, 74(7): 1281-1291. [Zheng Jingyun, Liu Yang, Wu Maowei, et al. Evidences and regional differences on multi-scales in Medieval Climate Anomaly over China[J]. *Acta Geographica Sinica*, 2019, 74(7): 1281-1291.]
- [6] 黄博津,余克服,陈特固. 过去2000年的特征气候时段及其影响因素[J]. *海洋地质与第四纪地质*, 2013, 33(1): 97-108. [Huang Bojin, Yu Kefu, Chen Tegu. Recent progress on specific climatic stages and driving forces over last 2000 years[J]. *Marine Geology & Quaternary Geology*, 2013, 33(1): 97-108.]
- [7] Wang Q, Cheng K, Zheng Z H, et al. Relationship between climate, environment, and anthropogenic activities in coastal North China recorded by speleothem $\delta^{18}\text{O}$ and $\delta^{13}\text{C}$ ratios in the last 1 ka [J]. *Climate of the Past Discussions*, 2017: 1-25.
- [8] Lan J H, Xu H, Lang Y C, et al. Dramatic weakening of the East Asian summer monsoon in northern China during the transition from the Medieval Warm Period to the Little Ice Age[J]. *Geology*, 2020, 48(4): 307-312.
- [9] Wang X H, Wang L S, Hu S Y, et al. Indian summer monsoon variability over last 2000 years inferred from sediment magnetic characteristics in Lugu Lake, Southwest China[J]. *Palaeogeography, Palaeoclimatology, Palaeoecology*, 2021, 578: 110581.
- [10] Zhang P Z, Cheng H, Edwards R L, et al. A test of climate, sun, and culture relationships from an 1810-year Chinese cave record [J]. *Science*, 2008, 322(5903): 940-942.
- [11] 陈朝军,袁道先,程海,等. 人类活动和气候变化触发了中国西南石漠化的扩张[J]. *中国科学(D辑): 地球科学*, 2021, 51(11): 1950-1963. [Chen Chaojun, Yuan Daoxian, Cheng Hai, et al. Human activity and climate change triggered the expansion of rocky desertification in the karst areas of southwestern China [J]. *Science China (Seri. D): Earth Sciences*, 2021, 51(11): 1950-1963.]

- [12] Chen J H, Chen F H, Feng S, et al. Hydroclimatic changes in China and surroundings during the Medieval Climate Anomaly and Little Ice Age: Spatial patterns and possible mechanisms[J]. *Quaternary Science Reviews*, 2015, 107: 98-111.
- [13] Zhang J W, Zhao K, Wang Y J, et al. Modulation of centennial-scale hydroclimate variations in the middle Yangtze River valley by the East Asian-Pacific pattern and ENSO over the past two millennia[J]. *Earth and Planetary Science Letters*, 2021, 576: 117220.
- [14] Hu C Y, Henderson G M, Huang J H, et al. Quantification of Holocene Asian monsoon rainfall from spatially separated cave records[J]. *Earth and Planetary Science Letters*, 2008, 266(3/4): 221-232.
- [15] Emile-Geay J, Cane M, Seager R, et al. El Niño as a mediator of the solar influence on climate[J]. *Paleoceanography*, 2007, 22(3): PA3210.
- [16] Fleitmann D, Burns S J, Mangini A, et al. Holocene ITCZ and Indian monsoon dynamics recorded in stalagmites from Oman and Yemen (Socotra)[J]. *Quaternary Science Reviews*, 2007, 26(1/2): 170-188.
- [17] Wang Y J, Cheng H, Edwards R L, et al. The Holocene Asian monsoon: Links to solar changes and North Atlantic climate[J]. *Science*, 2005, 308(5723): 854-857.
- [18] Liu D B, Wang Y J, Cheng H, et al. Strong coupling of centennial-scale changes of Asian monsoon and soil processes derived from stalagmite $\delta^{18}\text{O}$ and $\delta^{13}\text{C}$ records, southern China[J]. *Quaternary Research*, 2016, 85(3): 333-346.
- [19] Chen C J, Huang R, Yuan D X, et al. Karst hydrological changes during the Late-Holocene in southwestern China[J]. *Quaternary Science Reviews*, 2021, 258: 106865.
- [20] Jia W, Zhang P Z, Zhang L L, et al. Highly resolved $\delta^{13}\text{C}$ and trace element ratios of precisely dated stalagmite from northwestern China: Hydroclimate reconstruction during the last two millennia[J]. *Quaternary Science Reviews*, 2022, 291: 107473.
- [21] 白雨洁, 吴江滢, 梁怡佳, 等. 湖北玉龙洞石笋多指标记录的4.2 ka事件[J]. *第四纪研究*, 2020, 40(4): 959-972. [Bai Yujie, Wu Jiangying, Liang Yijia, et al. The multi-proxy record of a stalagmite from Yulong cave, Hubei during the 4.2 ka event[J]. *Quaternary Sciences*, 2020, 40(4): 959-972.]
- [22] Zhang H W, Cheng H, Sinha A, et al. Collapse of the Liangzhu and other Neolithic cultures in the Lower Yangtze region in response to climate change[J]. *Science Advances*, 2021, 7(48): ea-bi9275.
- [23] Zhao K, Wang Y J, Edwards R L, et al. Contribution of ENSO variability to the East Asian summer monsoon in the Late Holocene[J]. *Palaeogeography, Palaeoclimatology, Palaeoecology*, 2016, 449: 510-519.
- [24] Cui Y F, Wang Y J, Cheng H, et al. Isotopic and lithologic variations of one precisely-dated stalagmite across the Medieval/LIA Period from Heilong cave, central China[J]. *Climate of the Past*, 2012, 8(5): 1541-1550.
- [25] 何报寅, 张穗, 蔡述明. 近2600年神农架大九湖泥炭的气候变化记录[J]. *海洋地质与第四纪地质*, 2003, 23(2): 109-115. [He Baoyin, Zhang Sui, Cai Shuming. Climatic changes recorded in peat from the Dajiu lake basin in Shennongjia since the last 2600 years[J]. *Marine Geology & Quaternary Geology*, 2003, 23(2): 109-115.]
- [26] 张伟宏, 陈仕涛, 汪永进, 等. 小冰期东亚夏季风快速变化特征: 湖北石笋记录[J]. *第四纪研究*, 2019, 39(3): 765-774. [Zhang Weihong, Chen Shitao, Wang Yongjin, et al. Rapid change in the East Asian summer monsoon: Stalagmite records in Hubei, China[J]. *Quaternary Sciences*, 2019, 39(3): 765-774.]
- [27] 陈剑舜, 张伟宏, 陈仕涛, 等. 小冰期气候的湖北石笋碳同位素记录[J]. *沉积学报*, 2020, 38(3): 497-504. [Chen Jianshun, Zhang Weihong, Chen Shitao, et al. Carbon isotope record in stalagmites from Hubei during the Little Ice Age[J]. *Acta Sedimentologica Sinica*, 2020, 38(3): 497-504.]
- [28] Duan F C, Zhang Z Q, Wang Y, et al. Hydrological variations in central China over the past millennium and their links to the tropical Pacific and North Atlantic oceans[J]. *Climate of the Past*, 2020, 16(2): 475-485.
- [29] Wang Q, Wang Y J, Zhao K, et al. The transfer of oxygen isotopic signals from precipitation to drip water and modern calcite on the seasonal time scale in Yongxing cave, central China[J]. *Environmental Earth Sciences*, 2018, 77(12): 474.
- [30] 张伟宏, 廖泽波, 陈仕涛, 等. 湖北高分辨率石笋记录的DO18事件特征[J]. *沉积学报*, 2018, 36(4): 674-683. [Zhang Weihong, Liao Zebo, Chen Shitao, et al. DO18 event depicted by a high-resolution stalagmite record from Yongxing cave, Hubei province[J]. *Acta Sedimentologica Sinica*, 2018, 36(4): 674-683.]
- [31] Chen S T, Wang Y J, Cheng H, et al. Strong coupling of Asian Monsoon and Antarctic climates on sub-orbital timescales[J]. *Scientific Reports*, 2016, 6: 32995.
- [32] Cheng H, Sinha A, Wang X F, et al. The global paleomonsoon as seen through speleothem records from Asia and the Americas [J]. *Climate Dynamics*, 2012, 39(5): 1045-1062.
- [33] Hercman H, Pawlak J. MOD-AGE: An age-depth model construction algorithm[J]. *Quaternary Geochronology*, 2012, 12: 1-10.
- [34] Fohlmeister J. A statistical approach to construct composite climate records of dated archives[J]. *Quaternary Geochronology*, 2012, 14: 48-56.
- [35] Mudelsee M. Ramp function regression: A tool for quantifying climate transitions[J]. *Computers & Geosciences*, 2000, 26(3): 293-307.
- [36] Li Y D, Yang Y, Jiang X Y, et al. The transport mechanism of carbon isotopes based on 10 years of cave monitoring: Implications for paleoclimate reconstruction[J]. *Journal of Hydrology*,

- 2021, 592: 125841.
- [37] Baker A J, Matthey D P, Baldini J U L. Reconstructing modern stalagmite growth from cave monitoring, local meteorology, and experimental measurements of dripwater films[J]. *Earth and Planetary Science Letters*, 2014, 392: 239-249.
- [38] 孔兴功,汪永进,吴江滢. 南京葫芦洞石笋 $\delta^{13}\text{C}$ 对冰期气候的复杂响应与诊断[J]. *中国科学(D辑): 地球科学*, 2005, 35(11): 1047-1052. [Kong Xinggong, Wang Yongjin, Wu Jiangying, et al. Complicated responses of stalagmite $\delta^{13}\text{C}$ to climate change during the last glaciation from Hulu cave, Nanjing, China[J]. *Science China (Seri. D): Earth Sciences*, 2005, 35(11): 1047-1052.]
- [39] Liang Y J, Zhao K, Wang Y J, et al. Different response of stalagmite $\delta^{18}\text{O}$ and $\delta^{13}\text{C}$ to millennial-scale events during the last glacial, evidenced from Huangjin cave, northern China[J]. *Quaternary Science Reviews*, 2022, 276: 107305.
- [40] Fairchild I J, Smith C L, Baker A, et al. Modification and preservation of environmental signals in speleothems[J]. *Earth-Science Reviews*, 2006, 75(1/2/3/4): 105-153.
- [41] Wang Z J, Chen S T, Wang Y J, et al. Climatic implication of stalagmite $\delta^{13}\text{C}$ in the middle reaches of the Yangtze River since the Last Glacial Maximum and coupling with $\delta^{18}\text{O}$ [J]. *Palaeogeography, Palaeoclimatology, Palaeoecology*, 2022, 608: 111290.
- [42] Johnson K R, Hu C Y, Belshaw N S, et al. Seasonal trace-element and stable-isotope variations in a Chinese speleothem: The potential for high-resolution paleomonsoon reconstruction [J]. *Earth and Planetary Science Letters*, 2006, 244(1/2): 394-407.
- [43] Genty D, Blamart D, Ouahdi R, et al. Precise dating of Dansgaard-Oeschger climate oscillations in western Europe from stalagmite data[J]. *Nature*, 2003, 421(6925): 833-837.
- [44] 郜魁,何尧启,邱万银,等. 贵州黑洞4750年以来高分辨率石笋 $\delta^{13}\text{C}$ 记录[J/OL]. *沉积学报*, doi: 10.14027/j. issn. 1000-0550. 2022. 068. [Gao Kui, He Yaoqi, Qiu Wanyin, et al. A high-resolution stalagmite $\delta^{13}\text{C}$ record for the past 4 750 years from Dark cave, Guizhou, SW China[J/OL]. *Acta Sedimentologica Sinica*, doi: 10.14027/j. issn. 1000-0550. 2022. 068.]
- [45] 中央气象局气象科学研究所. 中国近五百年旱涝分布图集[M]. 北京: 地图出版社, 1981. [Chinese Academy of Meteorological Science CMA. Yearly charts of dryness/wetness in China for the last 500-year period[M]. Beijing: China Cartographic Publishing House, 1981.]
- [46] 谭明. 环流效应: 中国季风区石笋氧同位素短尺度变化的气候意义: 古气候记录与现代气候研究的一次对话[J]. *第四纪研究*, 2009, 29(5): 851-862. [Tang Ming. Circulation effect: Climatic significance of the short term variability of the oxygen isotopes in stalagmites from monsoonal China: Dialogue between paleoclimate records and modern climate research[J]. *Quaternary Sciences*, 2009, 29(5): 851-862.]
- [47] Zhang H W, Zhang X, Cai Y J, et al. A data-model comparison pinpoints Holocene spatiotemporal pattern of East Asian summer monsoon[J]. *Quaternary Science Reviews*, 2021, 261: 106911.
- [48] Zhang H W, Cai Y J, Tan L C, et al. Large variations of $\delta^{13}\text{C}$ values in stalagmites from southeastern China during historical times: Implications for anthropogenic deforestation[J]. *Boreas*, 2015, 44(3): 511-525.
- [49] Zhao M, Li H C, Shen C C, et al. $\delta^{18}\text{O}$, $\delta^{13}\text{C}$, elemental content and depositional features of a stalagmite from Yelang cave reflecting climate and vegetation changes since Late Pleistocene in central Guizhou, China[J]. *Quaternary International*, 2017, 452: 102-115.
- [50] Zhao J Y, Cheng H, Yang Y, et al. Role of the summer monsoon variability in the collapse of the Ming Dynasty: Evidences from speleothem records[J]. *Geophysical Research Letters*, 2021, 48(11): e2021GL093071.
- [51] 薛莲花,赵侃,崔英方,等. 近2000年来东亚夏季风突变的落水洞高分辨率石笋记录[J]. *第四纪研究*, 2020, 40(4): 973-984. [Xue Lianhua, Zhao Kan, Cui Yingfang, et al. Abrupt changes of East Asian summer monsoon over the past two millennia from stalagmite record in Luoshui cave, Hubei province [J]. *Quaternary Sciences*, 2020, 40(4): 973-984.]
- [52] Cosford J, Qing H R, Matthey D, et al. Climatic and local effects on stalagmite $\delta^{13}\text{C}$ values at Lianhua cave, China[J]. *Palaeogeography, Palaeoclimatology, Palaeoecology*, 2009, 280(1/2): 235-244.
- [53] Shi F, Lu H Y, Guo Z T, et al. The position of the Current Warm Period in the context of the past 22,000 years of summer climate in China[J]. *Geophysical Research Letters*, 2021, 48(5): e2020GL091940.
- [54] 邓云凯,李亮,马春梅,等. 江西玉山山泥炭2000 a BP以来的元素地球化学记录及其气候意义[J]. *地层学杂志*, 2019, 43(4): 352-363. [Deng Yunkai, Li Liang, Ma Chunmei, et al. The geochemical records and paleoclimate significance in peat from the Yuhua mountain in Jiangxi province since the last two millennia[J]. *Journal of Stratigraphy*, 2019, 43(4): 352-363.]
- [55] He F N, Yang F, Zhao C S, et al. Spatially explicit reconstruction of cropland cover for China over the past millennium[J]. *Science China (Seri. D): Earth Sciences*, 2023, 66(1): 111-128.
- [56] Xiao X Y, Yang X D, Shen J, et al. Vegetation history and dynamics in the middle reach of the Yangtze River during the last 1500 years revealed by sedimentary records from Taibai lake, China[J]. *The Holocene*, 2013, 23(1): 57-67.
- [57] Gu Y S, Wang H L, Huang X Y, et al. Phytolith records of the climate change since the past 15000 years in the middle reach of the Yangtze River in China[J]. *Frontiers of Earth Science*, 2012, 6(1): 10-17.
- [58] Tan L C, Cai Y J, An Z S, et al. Centennial-to decadal-scale monsoon precipitation variability in the semi-humid region, northern China during the last 1860 years: Records from stalagmites in Huangye cave[J]. *The Holocene*, 2011, 21(2): 287-296.

- [59] 张愈, 马春梅, 赵宁, 等. 浙江天目山千亩田泥炭晚全新世以来 Rb/Sr 记录的干湿变化[J]. 地层学杂志, 2015, 39(1): 97-107. [Zhang Yu, Ma Chunmei, Zhao Ning, et al. Late Holocene Rb/Sr ratios as a paleoclimate proxy in the Qianmutian peat of Tianmu mountains, Zhejiang province[J]. Journal of Stratigraphy, 2015, 39(1): 97-107.]
- [60] Moberg A, Sonechkin D M, Holmgren K, et al. Highly variable northern Hemisphere temperatures reconstructed from low-and high-resolution proxy data[J]. Nature, 2005, 433(7026): 613-617.
- [61] Ma C M, Zhu C, Zheng C G, et al. High-resolution geochemistry records of climate changes since late-glacial from Dajiuhe peat in Shennongjia mountains, central China[J]. Chinese Science Bulletin, 2008, 53(Suppl. 1): 28-41.
- [62] 李美娇, 何凡能, 杨帆, 等. 明代省域耕地数量重建及时空特征分析[J]. 地理研究, 2020, 39(2): 447-460. [Li Meijiao, He Fanneng, Yang Fan, et al. Reconstruction of provincial cropland area and its spatial-temporal characteristics in the Ming Dynasty [J]. Geographical Research, 2020, 39(2): 447-460.]
- [63] Sha L B, Jiang H, Seidenkrantz M S, et al. Solar forcing as an important trigger for West Greenland sea-ice variability over the last millennium[J]. Quaternary Science Reviews, 2016, 131: 148-156.
- [64] Bond G, Kromer B, Beer J, et al. Persistent solar influence on North Atlantic climate during the Holocene[J]. Science, 2001, 294(5549): 2130-2136.
- [65] Zhang Z Q, Liang Y J, Wang Y J, et al. Evidence of ENSO signals in a stalagmite-based Asian monsoon record during the Medieval Warm Period[J]. Palaeogeography, Palaeoclimatology, Palaeoecology, 2021, 584: 110714.
- [66] Steinhilber F, Beer J, Fröhlich C. Total solar irradiance during the Holocene[J]. Geophysical Research Letters, 2009, 36(19): L19704.
- [67] Shi F, Yang B, von Gunten L. Preliminary multiproxy surface air temperature field reconstruction for China over the past millennium[J]. Science China: Earth Sciences, 2012, 55(12): 2058-2067.
- [68] Tan L C, Shen C C, Löwemark L, et al. Rainfall variations in central Indo-Pacific over the past 2,700 y[J]. Proceedings of the National Academy of Sciences of the United States of America, 2019, 116(35): 17201-17206.
- [69] Moy C M, Seltzer G O, Rodbell D T, et al. Variability of El Niño/southern oscillation activity at millennial timescales during the Holocene Epoch[J]. Nature, 2002, 420(6912): 162-165.
- [70] Suess H E. The radiocarbon record in tree rings of the last 8000 years[J]. Radiocarbon, 1980, 22(2): 200-209.
- [71] Feng X X, Yang Y, Cheng H, et al. The 7.2 ka climate event: Evidence from high-resolution stable isotopes and trace element records of stalagmite in Shuiming cave, Chongqing, China[J]. The Holocene, 2020, 30(1): 145-154.
- [72] Chiang J C H, Bitz C M. Influence of high latitude ice cover on the marine intertropical convergence zone[J]. Climate dynamics, 2005, 25(5): 477-496.
- [73] Tan M. Circulation effect: Response of precipitation $\delta^{18}\text{O}$ to the ENSO cycle in monsoon regions of China[J]. Climate dynamics, 2014, 42(3/4): 1067-1077.
- [74] Yan H, Sun L G, Wang Y H, et al. A record of the southern oscillation index for the past 2,000 years from precipitation proxies[J]. Nature Geoscience, 2011, 4(9): 611-614.
- [75] Renssen H, Goosse H, Muscheler R. Coupled climate model simulation of Holocene cooling events: Oceanic feedback amplifies solar forcing[J]. Climate of the Past, 2006, 2(2): 79-90.

Rapidity of the Climatic and Environmental Changes During the Past Millennium Inferred from Stalagmite $\delta^{13}\text{C}$ Records in the Middle Reaches of the Yangtze River

LIU Jing¹, ZHANG WeiHong¹, XU Hao², SHAO QingFeng², LU HaiXin¹, LI MaoXia¹, CHEN JianShun²

1. College of Geography and Environment Science, Zhejiang Normal University, Jinhua, Zhejiang 321004, China

2. College of Geography Science, Nanjing Normal University, Nanjing 210023, China

Abstract: [Objective] This study examined the ecological and hydrological variability and regime shift during the Medieval Climate Anomaly (MCA) and Little Ice Age (LIA) in the middle reaches of the Yangtze River. This region is climatically governed by the Asian monsoon, with increased precipitation in summer and decreased in winter. Our study helps deepen our understanding of the history of the regional ecological and hydrological changes and their connections to the monsoon climate. [Methods] Based on two high-resolution stalagmite (YX262 and YX275) $\delta^{13}\text{C}$ records from Yongxing cave, Hubei province in the middle reaches of the Yangtze River, we reconstructed the history of the local paleoclimate and environment from 1 044-1 954 A.D. by creating a composite of the two records using the iscam program. [Results] The $\delta^{13}\text{C}$ records show two completely different states during the MCA and LIA, with the lower $\delta^{13}\text{C}$ values characterizing the MCA period, and the higher $\delta^{13}\text{C}$ values the LIA. During the transition from MCA to LIA, $\delta^{13}\text{C}$ shows an abrupt change. This phenomenon indicates a regime shift from a strong to weak state for the vegetation respiration activity and precipitation variation. This variation is consistent with many stalagmite $\delta^{13}\text{C}$ records in southwest China and the middle reaches of the Yangtze River. Here, our stalagmite $\delta^{13}\text{C}$ record shows that the shift of the vegetation cover was rapid from the MCA to LIA. A Rampfit analysis shows that the stalagmite $\delta^{13}\text{C}$ shift occurred between 1 434-1 460 A.D., lasting 26 years, which is more rapid and significantly longer than the stalagmite $\delta^{18}\text{O}$ shift. This variation is attributed to both climate deterioration and human activity influences, leading to a reduction of vegetation cover during this period. On the one hand, the rapid transformation of the stalagmite $\delta^{13}\text{C}$ record in Yongxing cave may be related to the great migration event in the early Ming Dynasty. A large number of migrants swarmed into Hubei province, inevitably leading to large-scale deforestation and land reclamation and changing the ecological environment of the surface soil vegetation. Those behaviors cause positive stalagmite $\delta^{13}\text{C}$. On the other hand, the Yongxing $\delta^{13}\text{C}$ record is correlated with changes in the total solar radiation, intertropical convergence zone (ITCZ), temperature in eastern China, and El Niño-Southern Oscillation (ENSO) on the MCA and LIA event scales. During the MCA period, the total solar irradiance was larger, and the ITCZ was farther north, with a high frequency of El Niño states. However, during the LIA period, the total solar irradiance was relatively small, and the position of ITCZ was more southerly, in the low frequency period of El Niño states. This correlation indicates that the changes of hydrological circulation and vegetation cover in the middle reaches of the Yangtze River had a dynamic relationship with the regional and global climate change during the past millennium, and the impacts of human activities on surface vegetation may be related to the background of regional or global climate change. [Conclusions] By studying the $\delta^{13}\text{C}$ record of stalagmites in Yongxing cave in the past millennium, the eco-hydrological characteristics of MCA and LIA were found to be significantly different, which may be related to global climate change and human activities. The study not only clearly establishes the time boundary between MCA and LIA in the middle reaches of the Yangtze River, but also deepens our understanding of the characteristics and causes of eco-hydrological environment changes in the region during the two periods.

Key words: stalagmite; carbon isotope; surface vegetation; transformation; LIA